

Coherence of wind pressure on domes

Nyi Nyi Aung Ye Jihong

(Key Laboratory of Concrete and Prestressed Concrete Structure of Ministry of Education, Southeast University, Nanjing 210096, China)

Abstract: The concept of the coherence function is adopted to find the wind pressure correlation of two points on domes of different rise-span ratios. The pressure measurements are made on the dome roof models by the wind tunnel test. The coherence functions for different separation distances at several directions of the domes from different wind directions are examined. The results show that there is a strong correlation for two adjacent points at low frequency, but not for non-adjacent points. The coherence of the wind pressure increases with the decrease in the separation distance. Moreover, the coherence of the wind pressure is in the strongest correlation on the along-wind direction at the same separation, but the lowest correlation is on the cross-wind direction. The detailed derivation of the proposed exponential coherence model of the wind pressure from experimental data is also discussed. It is found that the proposed exponential coherence model can be appropriate, especially, for small separations and the change in the directions on domes. Based on the quasi-steady theory, the relationship between the wind pressure and the wind velocity on the basis of the coherence model is also examined. The coherence observed between the wind pressure and the wind velocity is not adequately predicted by the quasi-steady theory.

Key words: domes; coherence of wind pressure; exponential coherence model of wind pressure; quasi-steady theory

Domes provide an easy and economic method of large areas of the roof and they are frequently used by the designers who realize the advantages and the elegant beauty of the construction^[1]. Since the wind pressures on domes vary spatially as well as in time, the design wind loads should be determined by considering the dynamic characteristics of wind pressures^[2]. Long-span and lightweight roofs, such as spherical pneumatic domes, tend to vibrate in strong winds^[3]. In other words, wind loads have a significant proportion of the total load acting on such structures and so the magnitude and distribution of the resultant pressures must be considered^[4]. Ogawa et al.^[5] experimentally investigated the time-space correlation of the wind pressures in a wind tunnel and constructed a simple model of the pressure field. Hongo^[6-7] carried out a series of wind-tunnel experiments on the mean and fluctuating wind pressures by investigating the effects on the turbulence of the approaching flow and the geometry of domes on the characteristics of the pressure field. Many researches have been focused on the coherence of the wind pressure on the spherical domes. Mo-

reover, many wind loading standards employ a quasi-steady approach for the design of structures. Unfortunately, many studies conclude that the quasi-steady theory cannot properly predict the coherence of the wind pressure and the coherence of the wind velocity^[8-9].

1 Fitting Method of Coherence Function of Wind Pressure

A mathematical definition of the magnitude-squared coherence function, $\gamma_{ij}^2(f)$, of two stationary random processes, i and j , can be given as

$$\gamma_{ij}^2(f) = \frac{|S_{ij}(f)|^2}{S_{ii}(f)S_{jj}(f)} \quad (1)$$

where $S_{ii}(f)$ and $S_{jj}(f)$ are the auto-sided power spectral density function of i and j , respectively, at frequency f ; $S_{ij}(f)$ is the one-sided complex-valued cross-power spectral density function between the two processes. The coherence $\gamma_{ij}^2(f)$ is always greater than or equal to zero and less than or equal to one.

1.1 Numerical studies

In this section, the frequency of interest, the influence of separation distances and the influence of direction are studied to estimate good coherence spectra. To achieve good estimates of coherence spectra, it is necessary to define the appropriate testing points and choose an appropriate pair of testing points on structures. Based on the wind tunnel pressure test, we can symmetrically obtain the wind pressure time-history testing points of the whole surface of domes as shown in Fig. 1. The coherence function of different separations of the dome ($f: l = 1:2$) is briefly studied along 0° , 30° , 60° , 90° directions and so on. But, for the dome ($f: l = 1:5$), the coherence function is only studied along 0° , 45° , -45° and 90° directions, because the suitable pairs of testing points on domes can be obtained along these directions (see Fig. 1).

1.2 Smooth technique

It must be noticed that the experimental data should not be fitted after smoothing, because the act of smoothing invalidates the assumption that the errors are normally distributed^[10]. A data smoothing of the coherence curve is carried out in this paper in order to study the influence of both frequency and separation distance to obtain the coherence function. Fig. 2 and Fig. 3 show the coherence functions for adjacent points and non-adjacent points on all the directions of domes. Moreover, coherence functions are clearly dependent on the separation distances and the angles of direction, as shown in Tab. 1.

Received 2009-08-05.

Biographies: Nyi Nyi Aung (1978—), male, graduate; Ye Jihong (corresponding author), female, doctor, professor, yejihong@seu.edu.cn.

Foundation item: The National Natural Science Foundation of China (No. 50678036).

Citation: Nyi Nyi Aung, Ye Jihong. Coherence of wind pressure on domes[J]. Journal of Southeast University (English Edition), 2010, 26 (1): 100–106.

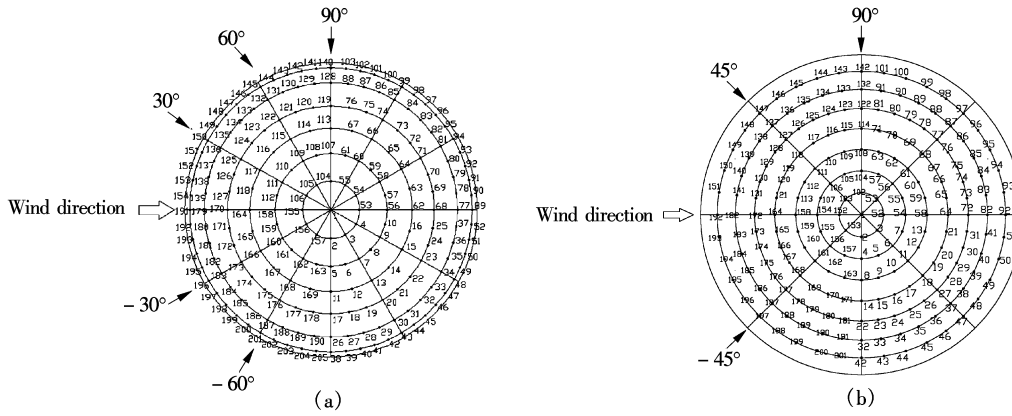


Fig. 1 Wind tunnel testing points on domes. (a) Testing points on dome ($f:l=1:2$) (b) Testing points on dome ($f:l=1:5$)

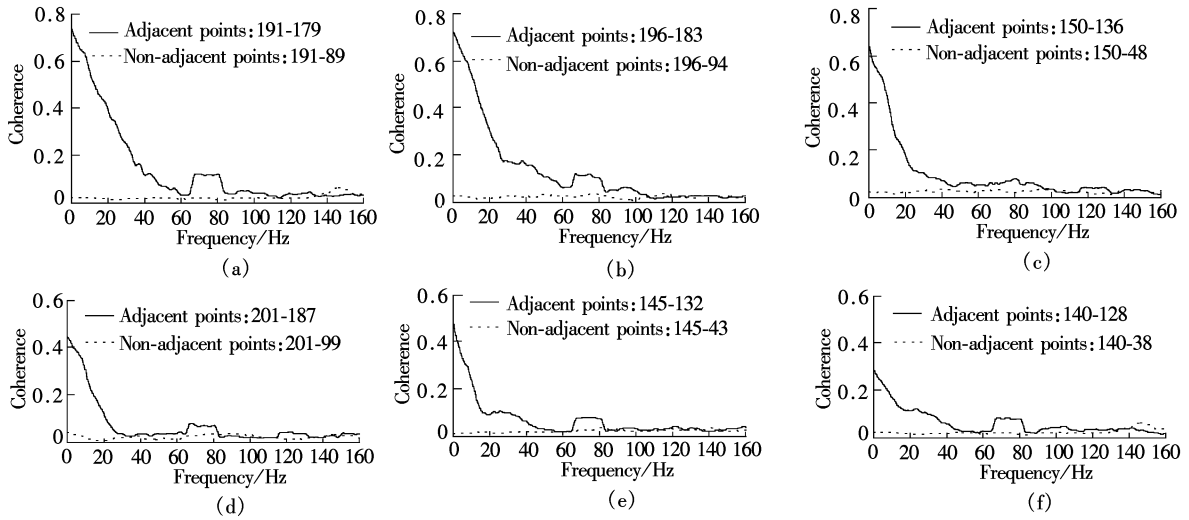


Fig. 2 Coherence function of wind pressure of dome ($f:l=1:2$). (a) 0° ; (b) -30° ; (c) 30° ; (d) -60° ; (e) 60° ; (f) 90°

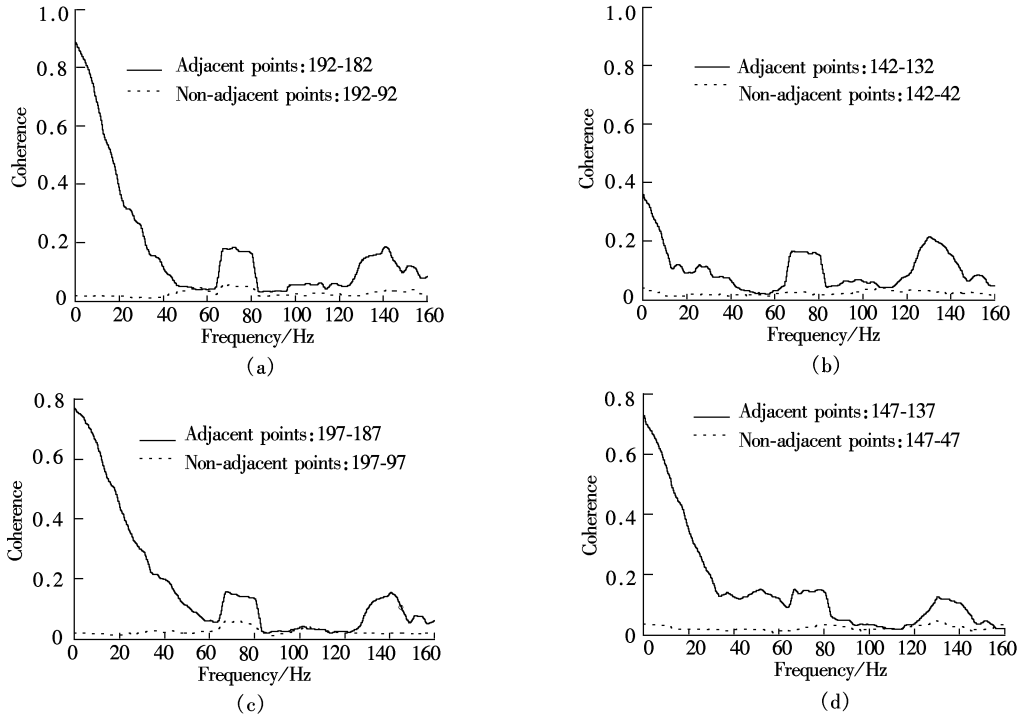


Fig. 3 Coherence function of wind pressure of dome ($f:l=1:5$). (a) 0° ; (b) 90° ; (c) -45° ; (d) 45°

Tab. 1 Values of coherence function of different separations of 0° direction on domes

$f:l=1:2$				$f:l=1:5$			
Pair of points	L/m	Coherence (largest)	Remark	Pair of points	L/m	Coherence (largest)	Remark
191-179	13.048 77	0.742 44		192-182	6.890 142	0.889 53	
191-170	25.872 68	0.490 82		192-172	13.764 72	0.784 04	
191-164	35.226 59	0.345 02	Right-side	192-164	20.608 19	0.624 58	Right-side
191-158	44.206 11	0.279 23	of dome	192-158	27.405 11	0.493 67	of dome
191-155	52.788 02	0.195 82	(windward)	192-154	34.140 11	0.384 59	(windward)
191-1	60.855 46	0.018 14		192-152	40.797 98	0.292 98	
				192-1	47.363 68	0.007 59	
191-53	68.337 36	0.025 03		192-52	53.822 37	0.017 49	
191-56	75.263 29	0.024 14		192-54	60.159 46	0.016 56	
191-62	81.263 28	0.022 90	Left-side	192-58	66.360 64	0.014 66	Left-side
191-68	86.582 58	0.021 23	of dome	192-64	72.411 89	0.011 57	of dome
191-77	92.372 13	0.025 95	(leeward)	192-72	78.299 54	0.014 13	(leeward)
191-89	96.582 50	0.023 75		192-82	84.010 29	0.014 09	
				192-92	89.531 26	0.018 73	

Tab. 1 gives the characteristics of the coherence function of different separations of 0° direction on domes. On the windward portion, the largest values of coherence functions decrease with the increase in separation distances. On the other hand, all the largest values of coherence functions on the leeward portion are nearly constant and approach zero. Therefore, it can be concluded that coherences clearly show the relationship between the separation distances of two points and the coherence function.

The values of the coherence function for all the directions

are shown in Tab. 2. It is found that the value of the coherence function of 0° direction is the largest for all the angles of directions (0° direction is also called the wind direction), but the smallest value is in the 90° direction. And then, different values of the coherence function at (30°, -30°) are a bit large, but they are nearly equal at (45°, -45°) and (60°, -60°). Therefore, it can be seen that it obeys the symmetry of directions and different separation distances.

Tab. 2 Values of coherence function of all the directions on domes

$f:l=1:2$				$f:l=1:5$			
Angle from wind direction	Pair of points	L/m	Coherence (largest)	Angle from wind direction	Pair of points	L/m	Coherence (largest)
0°	191-179	13.048 77	0.742 44	0°	192-182	6.890 14	0.889 53
30°	150-136	13.048 77	0.652 45	45°	150-136	6.890 14	0.737 96
-30°	196-183	13.048 77	0.728 30	-45°	197-187	6.890 14	0.776 21
60°	145-132	13.048 77	0.488 39	90°	142-132	6.890 14	0.369 37
-60°	201-187	13.048 77	0.453 30				
90°	140-128	13.048 77	0.290 44				

1.3 Derivation of proposed coherence model of wind pressure

There is very little literature on the coherence model of wind pressure. Some empirical models of wind velocity fail to account for reduction in coherence at low frequencies and large separations^[11-12]. To account for such limitations, in this section, an exponential coherence model is proposed and it is also empirically based. Using the least-square fitting method, the two-term exponential model, $y = ae^{bx} + ce^{dx}$, gives a better statistical fit than other models^[13]. In this model, frequency of interest, separation distances and angle of direction might be emphasized, which allows for reduction in coherence with the increase in separation and the change in the angles of direction. This exponential coherence model can be expressed as

$$\gamma_{ij}^2(f, L_{ij}, \theta) = \left\{ ah \cos\left(\frac{\theta}{2}\right) \exp(bf)^{1/4} + ch \cos\left(\frac{\theta}{2}\right) \exp(df)^{1/4} \right\}^2 \quad (2)$$

where h is denoted by $(D - L_{ij})/D$ and $L_{ij} = \sqrt{[(x_j - x_i)^2 + (y_j - y_i)^2 + (z_j - z_i)^2]}$. Here, L_{ij} is the separation distance of two testing points at points i and j ; (x_i, y_i, z_i) and (x_j, y_j, z_j) are coordinates at points i and j ; f is frequency of interest; θ is the angle of the direction from the wind direction; and D is the span of the dome. Parameters a , b , c and d can be estimated from estimates of coherence spectra by only using the experimental data of the dome ($f:l=1:2$). In the next section, the new coherence model can be compared with the coherence spectra of the dome ($f:l=1:5$). Hereinafter, it is shown that these parameters cannot be estimated from smoothing coherence spectra. For illustration purposes, data from all the directions and separation distances between testing points are used. Totally 300 pairs of points are considered in this research. To employ all of the data and estimate the parameters a , b , c and d is of greater interest. The parameters a and c are mostly greater than or equal to zero and always less than unity. But, the decay parameters b and d are mostly less than or equal to zero and always negative.

From Fig. 4(a) and Fig. 4(c), the values of parameters a and c increase as the separation distances shorten and decrease when the separation distances lengthen. But, the parameters b and d are not dependent on the separation distances and these values mostly approach zero (see Fig. 4(b) and Fig. 4(d)). Therefore, it can be seen that the parameters a and c have a relationship with separation distances and changes in the angles of directions. When these param-

eters are estimated, unacceptable coefficients obtained from using least-squares fit can be removed from the estimation of parameters. For each separation and angle of direction, over a range of frequencies of interest from 0 to 168 Hz, the overall least-squares fit parameters a , b , c and d for the exponential model for the coherence function are 0.865 6, -0.103 7, 0.185 2 and -0.015 2, respectively, based on data recorded over 300 pairs of points (see Fig. 4).

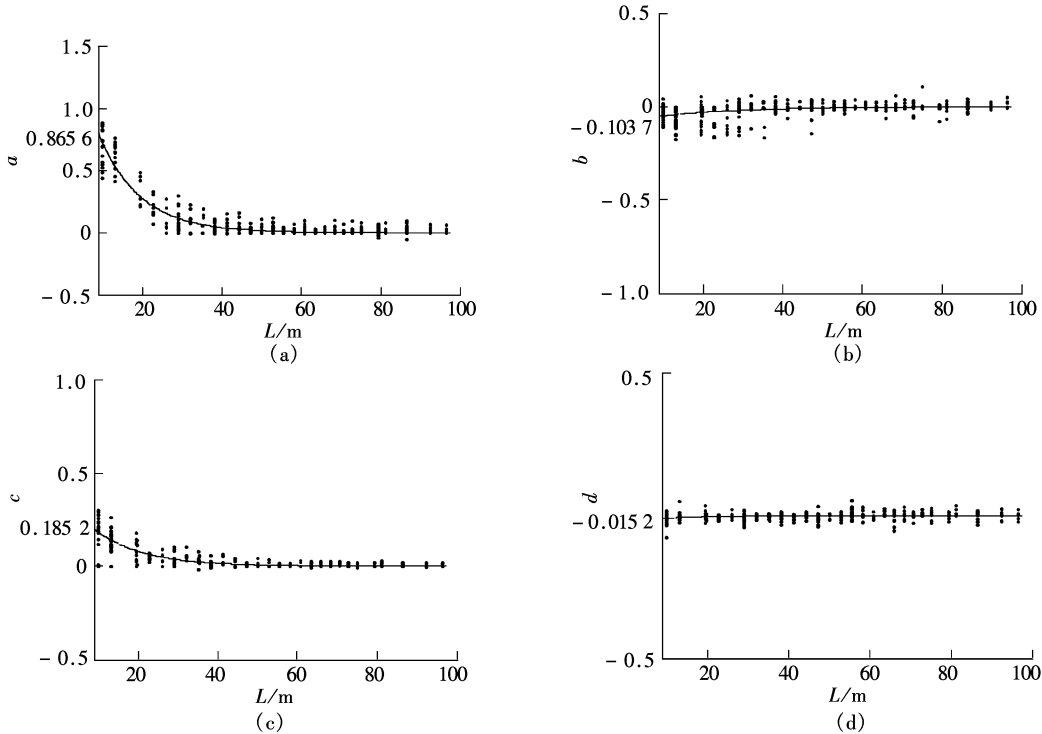


Fig. 4 Estimated parameters for proposed exponential coherence model using totally 300 pairs of points from all directions on the dome ($f:l=1:2$). (a) Parameter a ; (b) Parameter b ; (c) Parameter c ; (d) Parameter d

In a derivation of a proposed exponential coherence model, parameter a is the main value to reach the goal of derivation because it can give a good exponential curve feature compared with coherence spectra using experimental data in this research.

1.4 Discussion on proposed coherence model of wind pressure on domes

1.4.1 Comparing coherence function of dome ($f:l=1:2$) with proposed coherence model

It can be proposed that the smoothing coherence spectra of each direction are used to be compared with a proposed coherence model. Moreover, it can also be seen that the proposed coherence model can be compared with any coherence spectra if the coherence curve obtained from the data is reasonable in any direction and at any separation distance.

From Fig. 5, coherences of the proposed exponential model for all the directions decrease with the increased separation at all the frequencies. At any separation, it can be seen that the coherence at 0° direction is the strongest for all the directions while the coherence at diagonal directions such as 30° , -30° , 60° and -60° directions is in considerably strong correlation. The coherence in the 90° direction is in the smallest correlation for all the directions. It can also

be seen that coherences in diagonal directions obey the rule of symmetry of directions.

1.4.2 Comparing coherence function of dome ($f:l=1:5$) with proposed coherence model

As has been already discussed in Fig. 3, the estimated coherence spectra of dome ($f:l=1:5$) in all the directions can be decreased with the increased separation distances. From Fig. 6, it is found that the coherence of small separation is in good correlation but the coherence of large separation is in poor correlation. Nevertheless, from the comparison of all the coherence functions, the results also show that the estimated coherence function of the wind pressure can be predicted by the proposed exponential coherence model.

1.4.3 Comparing coherence of the wind pressure with coherence of wind velocity

In this section, the coherence functions of the wind pressure and the wind velocity on domes are analyzed in order to verify the quasi-steady theory. The Davenport exponential coherence model^[14-15] is as

$$r_{ij}^2(x_i, y_i, z_i; x_j, y_j, z_j; n) = e^{-2h} \quad (3)$$

where h is denoted by

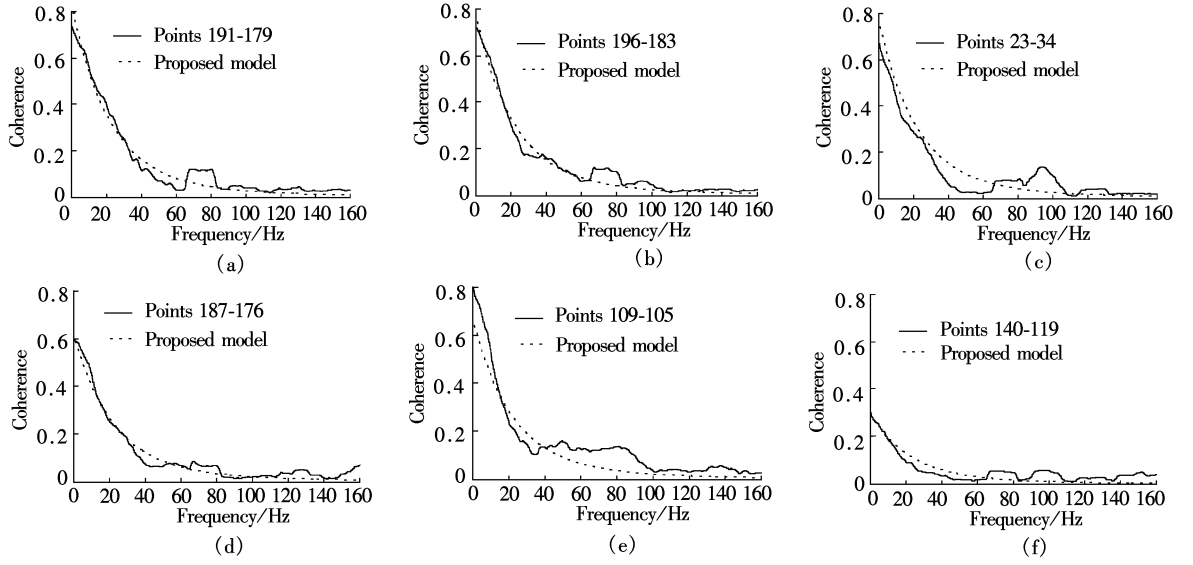


Fig. 5 Comparison of coherence spectra with proposed exponential coherence model using random two points of all directions on dome ($f: l = 1: 2$). (a) 0° ; (b) -30° ; (c) 30° ; (d) -60° ; (e) 60° ; (f) 90°

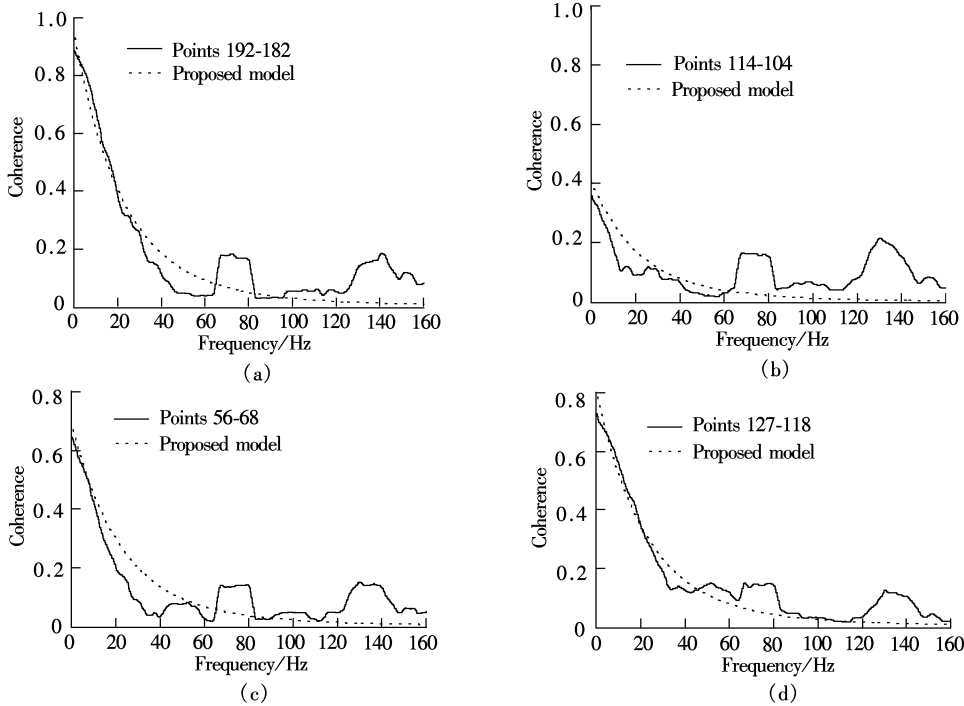


Fig. 6 Comparison of coherence spectra with proposed exponential coherence model using random two points of all the directions on dome ($f: l = 1: 5$). (a) 0° ; (b) 90° ; (c) -45° ; (d) 45°

$$\frac{n[c_x^2(x_i - x_j)^2 + c_y^2(y_i - y_j)^2 + c_z^2(z_i - z_j)^2]^{1/2}}{\frac{1}{2}[\bar{v}(z_i) + \bar{v}(z_j)]}$$

where (x_i, y_i, z_i) and (x_j, y_j, z_j) are coordinates i and j , respectively; $\bar{v}(z_i)$ and $\bar{v}(z_j)$ are the mean velocity of the height at i and j , respectively; c_x , c_y and c_z are 16, 18 and 10, respectively; n is the reduced frequency and defined as $n = fH/U_H$. f is the frequency of interest. H is the height of the top point of the model, $H = 40$ cm and U_H is the mean velocity of the height, $U_H = 10.44092$ m/s.

From Fig. 7, in the range between $f' = 0.01$ and 0.1 , the coherence of the proposed model of the wind pressure is higher than the coherence of the wind velocity given by

Eq. (3); and from Fig. 8, in the range between $f' = 0.05$ and 0.5 , the coherence of the proposed model of the wind pressure is also higher than the coherence of the wind velocity. Otherwise, at the range of low frequency, the coherence of the wind velocity is higher than the coherence of the wind pressure. Therefore, it can be concluded that the quasi-steady theory cannot properly predict the coherence of the wind pressure on domes.

2 Conclusions

1) At low frequency, the coherence function is in quite strong correlation for adjacent points, but it is in very weak correlation for two non-adjacent points; in addition, at high frequency, the coherence function is in quite weak correlation

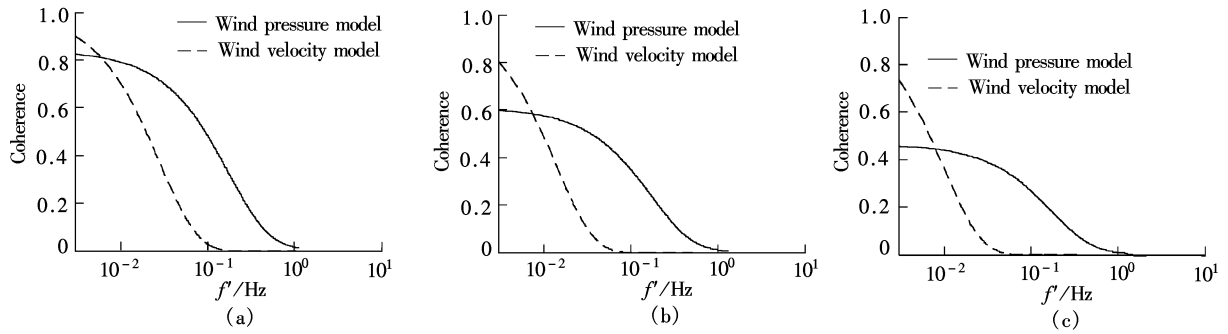


Fig. 7 Comparison of coherence models of wind pressure and wind velocity using different separations of dome ($f:l = 1:2$).
 (a) $L = 13.04877$ m; (b) $L = 25.87269$ m; (c) $L = 35.22659$ m

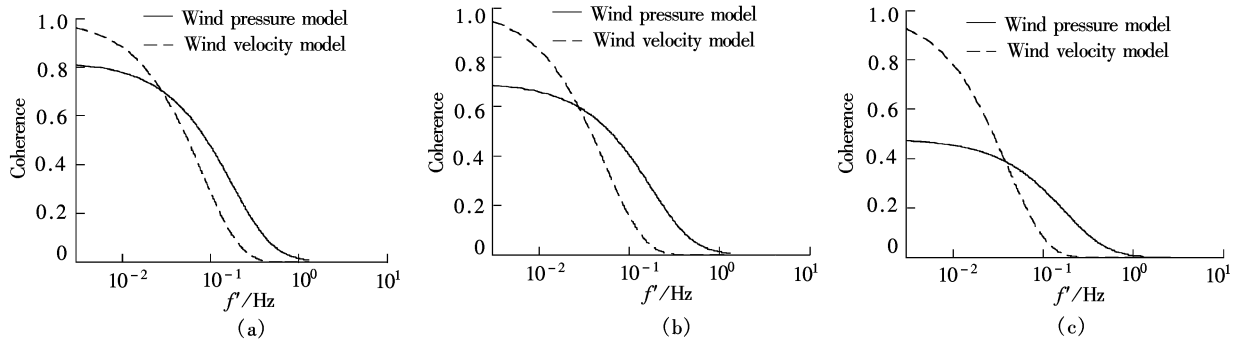


Fig. 8 Comparison of coherence models of wind pressure and wind velocity using different separations of dome ($f:l = 1:5$).
 (a) $L = 13.76472$ m; (b) $L = 20.60819$ m; (c) $L = 27.4051$ m

tion for any two points. The coherence of the wind pressure increases with the decrease in the separation distance. At the same separation distance, the coherence of the wind pressure on the along-wind direction is in the strongest correlation, while the coherence at the diagonal wind direction is in considerably strong correlation. But, the coherence at the across-wind direction is in the lowest correlation.

2) Based on the wind pressure time-history experimental data (totally 300 pairs of points) of the dome with a rise-span ratio ($f:l = 1:2$), a coherence function expression is fitted by the least-squares method to obtain a proposed coherence model, and compared with the experimental data of domes with rise-span ratios ($f:l = 1:2$) and ($f:l = 1:5$). The results show the valid estimates of the coherence spectra with the proposed coherence model. But, the coherence function of the proposed model loses valid estimates at large separation and low frequency.

3) In the process of comparing the coherence of the proposed model of the wind pressure with the exponential coherence of the wind velocity defined by Davenport, it is found that the quasi-steady theory also cannot properly predict the coherence of the wind pressure on domes.

References

- [1] Subramanian N. *Principles of space structures* [M]. New Delhi: Wheeler Publishing, 1999: 25–68.
- [2] Uematsu Yasushi, Tsuruishi Raku. Wind load evaluation system for the design of roof cladding of spherical domes [J]. *Journal of Wind Engineering and Industrial Aerodynamics*, 2008, **96**(10/11): 2054–2066.
- [3] Ogawa T, Nakayama M, Murayama S, et al. Characteristics of wind pressure on basic structures with curved surfaces and their response in turbulent flow [J]. *Journal of Wind Engineering and Industrial Aerodynamics*, 1991, **38**(2/3): 427–438.
- [4] Lechford C W, Sarkar P P. Mean and fluctuating wind loads on rough and smooth parabolic domes[J]. *Journal of Wind Engineering and Industrial Aerodynamics*, 2000, **88**(1): 101–117.
- [5] Ogawa T, Nakayama M, Murayama S. Characteristics of wind pressure on spherical domes and response of domes in turbulent flow [J]. *Journal of Structure and Construction Engineering*, 1989, **404**(2/3): 95–102.
- [6] Hongo T. Experimental study of wind pressure forces on spherical roofs [D]. Tohoku: Tohoku University, 1995: 18–25.
- [7] Cook N J. *The designer's guide to wind loading of building structures, part 2: static structures*[M]. London, UK: Butterworths, 1990: 8–24.
- [8] Geurts C P W. Full-scale and wind tunnel measurements of the wind and wind-induced pressure over suburban terrain [J]. *Journal of Wind Engineering and Industrial Aerodynamics*, 1996, **64**(2/3): 89–100.
- [9] Geurts C P W, Rutten H S, Wisse J A. Spectral characteristics of wind induced pressures on a full scale building in suburban terrain [J]. *Journal of Wind Engineering and Industrial Aerodynamics*, 1997, **69**(71): 609–618.
- [10] *The MathWorks curve fitting toolbox for use with Matlab, user's guide* [M]. Natick, MA, USA: The MathWorks, 2002: 23–45.
- [11] Korn S, Lance M, Paul S V. A comparison of standard coherence models for inflow estimates from field measurements [J]. *Journal of Solar Energy Engineering*, 2004, **126**(4): 1069–1082.
- [12] Geurts C P W, Rutten H S, Wisse J A. Coherence of wind-induced pressure on buildings in urban areas: set up of a full-scale experiment [J]. *Journal of Wind Engineering and Industrial Aerodynamics*, 1996, **65**(1/2/3): 31–41.
- [13] Li Yongle, Liao Haili, Qiang Shizhong. Weighting ensemble least-square method for flutter derivatives of bridge [J]. *Journal of Wind Engineering and Industrial Aerodynamics*, 2003, **91**(6): 713–721.

[14] Simiu E, Scanlan R H. *Wind effects on structures* [M]. 2nd ed. New York: Wiley, 1986: 60–98.

[15] Irwin P A. Bluff body aerodynamics in wind engineering [J]. *Journal of Wind Engineering and Industrial Aerodynamics*, 2008, **96**(6/7): 701–712.

球壳结构风压相关性研究

尼尼昂 叶继红

(东南大学混凝土与预应力混凝土结构教育部重点实验室, 南京 210096)

摘要: 引入相关函数以描述不同矢跨比的球壳上 2 点间的风压相关性. 根据风洞试验的风压测量数据, 研究了 2 点间距离不同、2 点连线与风向间角度不同时相干函数的大小. 结果表明球壳结构上毗邻的 2 点在低频段具有强相关性, 而非相邻点的风压相关性不明显. 风压相关性随 2 点距离的减小而增大. 距离相同时, 风压相关性在顺风向最强, 在横风向最弱. 根据风洞试验数据, 提出了球壳结构风压相关性指数模型, 并给出了确定该模型的详细过程. 结果表明该指数相关函数模型能恰当地描述距离较近 2 点间的相关性, 且能较好地反映风向角变化的影响. 此外, 根据准定常理论对风压、风速间的相关性进行了研究, 结果表明准定常理论对球壳结构风压、风速间的相关性不适用.

关键词: 球壳; 风压相关性; 风压指数相关函数模型; 准定常理论

中图分类号: TU391